Journal of Physics: Conference Series **217** (2010) 012143 doi:10.1088/1742-6596/217/1/012143

Dynamics of ferrocene in molecular sieves probed by Mössbauer spectroscopy and nuclear resonant scattering

T Asthalter[1], I Sergueev[2], U van Bürck[3], F E Wagner[3], P Härter[4], J Kornatowski[5], S Klingelhöfer[6] and P Behrens[6]

[1] (formerly) Institut für Physikalische Chemie, Universität Stuttgart, D–70569 Stuttgart, Germany

[2] European Synchrotron Radiation Facility, F–38043 Grenoble, France

[3] Experimentalphysik E13, Technische Universität München, D–85747 Garching, Germany

[4] Anorganische Chemie, Technische Universität München, D–85747 Garching, Germany

[5] Max-Planck-Institut für Kohlenforschung, D–45470 Mülheim, Germany

[6] Anorganische Chemie, Leibniz-Universität Hannover, D–30167 Hannover, Germany

E-mail: `t.asthalter@ipc.uni-stuttgart.de`

Abstract. A detailed study on the slow dynamics of ferrocene in the unidimensional channels of the molecular sieves SSZ–24 and $AlPO_4$–5 has been carried out, using Mössbauer spectroscopy (MS), nuclear forward scattering (NFS) and synchrotron radiation-based perturbed angular correlations (SRPAC). In both host systems, anisotropic rotational dynamics is observed above 100 K. For SSZ-24, this anisotropy persists even above the bulk melting temperature of ferrocene.

Various theoretical models are exploited for the study of anisotropic discrete jump rotations for the first time. The experimental data can be described fairly well by a jump model that involves reorientations of the molecular axis on a cone mantle with an opening angle dependant on temperature.

1. Introduction

The dynamics of guest molecules in zeolitic and related nanoporous hosts continues to be of current interest, as the catalytic and separation properties of zeolites critically depend on guest-molecule diffusion and host-guest interactions. A deeper insight into molecular motion in complex channel systems is only possible if the elementary dynamics in simple ordered host structures has been fully understood.

Rotation of guest molecules in zeolites is generally not isotropic because of the anisotropy of the host cage and of the guest molecule, but also – in the case of large cages – because the existence of different interstitial adsorption sites breaks the symmetry of the intermolecular potential of the guest molecule [1, 2].

The novel technique of nuclear resonant scattering (NRS) of synchrotron radiation comprises several different methods, such as nuclear forward scattering (NFS), nuclear inelastic scattering (NIS), and synchrotron radiation-based perturbed angular correlations (SRPAC). In particular, an immediate simultaneous observation of translational and rotational dynamics is now feasible

with the advent of the SRPAC technique [3], which is sensitive to relaxation of the hyperfine levels of the nuclear excited state and covers a dynamical range for rotational dynamics of more than five orders of magnitude. MS and NFS are selective to both the translational and the rotational motions of molecules containing a Mössbauer nucleus, on the timescale of the natural nuclear lifetime (141.1 ns for ^{57}Fe), whereas SRPAC is sensitive to rotational motion only.

In a previous study [4], a pioneering measurement of NFS spectra of ferrocene in oriented single crystals of $AlPO_4$-5 was carried out, and the presence of anisotropic rotation above 150 K could be inferred from the appearance of two quantum beats in the NFS spectrum. Rotational jump models [5] where the molecular electric field gradient jumps between the Cartesian axes only, did not reproduce the experiment quantitatively; also, they do not take the hexagonal symmetry of the host framework into account.

Here, we assess briefly the potential of MS and NRS for determining molecular anisotropic rotation at the example of ferrocene in SSZ-24 (for more details and the $AlPO_4$-5 data, see [6]).

Section 2 is a brief summary of existing rotational jump models in Mössbauer spectroscopy, to their extension by jump models based on Blume theory [7], and to a comparison with a recently developed jump model [8] (random jump cone or RJC model). Sample preparation, characterization, and experiments are described in Section 3. Section 4 presents a comparative view of Mössbauer and nuclear resonant scattering data at the example of SSZ-24 loaded with ferrocene. The results are summarized in Section 5.

2. Rotational jump models

For the ^{57}Fe transition, any molecule possessing an electric field gradient (EFG) will exhibit a two-line Mössbauer spectrum, corresponding to a single quantum beat (QB) in time domain. Reorientation of the ferrocene molecule within the nuclear lifetime leads to a decrease of the effective EFG tensor seen by the nucleus and thus to a complete or partial collapse of the two-line pattern of an ensemble of nuclei at rest.

The influence of pure spin dynamics (EFG rotation and/or electronic relaxation), where the stochastic motion occurs between discrete states, was treated in the general formalism of Blume [7]. For equally probable rotational jumps in the direction of the three Cartesian axes (Blume-Tjon model [9]), a simple closed solution exists. For different jump probabilities in the three Cartesian directions [5], more complicated analytical solutions were found that work well for crystal structures with symmetries up to orthorhombic. For completely random angular jumps [10] (strong-collision model or random phase approximation), the result is identical to that for the Blume-Tjon model [9].

[5] speculates that for 120° jumps "the relaxation produced will differ only in minor detail" from the 90° jump models. As a one-dimensional channel has a cylindrically restricted geometry, it is realistic to assume that the molecular axis, i.e. the electric field gradient, of the ferrocene will orient on a cone mantle within a preferred or maximal polar angle ϑ. The host systems of our study possess a local hexagonal symmetry. To the authors' knowledge, no attempts were reported to treat rotational jumps having this symmetry. Such an analysis has now been done within the frame of Blume theory, for mathematical details see [6]. It was assumed that the EFG main axis can orient on a cone mantle with an opening angle ϑ of 90°, 60° and 30° (90° corresponding to in-plane reorientations of the EFG), undergoing azimuthal jumps with 3- or 6-fold symmetry, see Fig. 1. Note that models A and B yield the same line shape, as orientations that differ by 180° can not be distinguished for a tensor of second rank. For the jump matrix, it was assumed that each orientation can be reached only *via* jumps from the neighbouring orientations, i. e. that only azimuthal jumps of 120° (3-jump) or 60° (6-jump) are allowed at any moment. All jump probabilities were set to the same value, corresponding to equally deep potential well minima.

As shown in Fig. 2, an increasing jump rate always leads to an initial asymmetric line

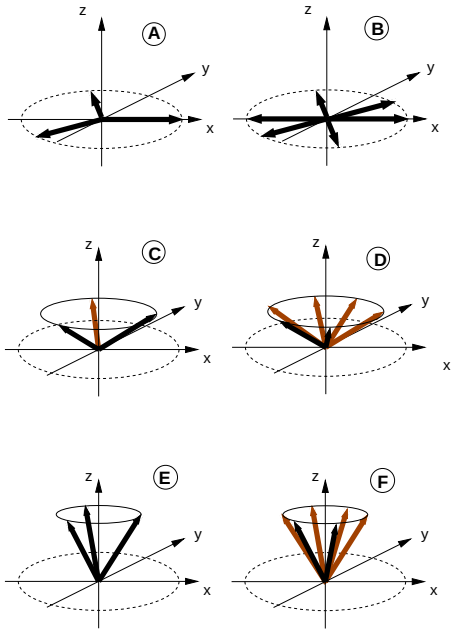

Figure 1. Orientation of the EFG tensor for the Blume jump models. The thick arrows show the possible orientations of the fivefold molecular axis of ferrocene, which coincides with the EFG tensor main axis.

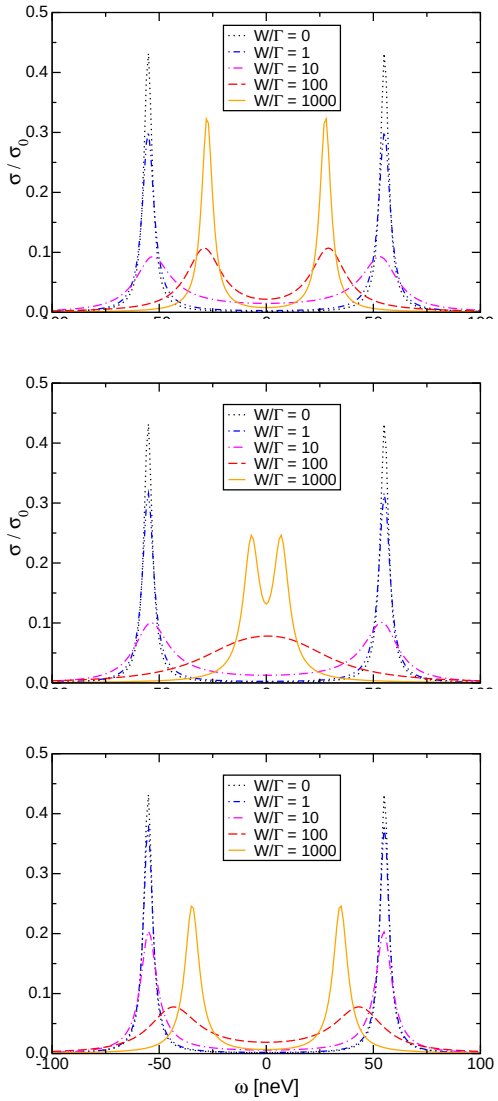

Figure 2. Theoretical Mössbauer absorption cross-section for jump models B (top), D (centre) and F (bottom). Relaxation rates W are in units of the natural line width ($\Gamma = 7.087\,\mathrm{MHz}$ for the ^{57}Fe resonance).

broadening, which is stronger towards the centre of the spectrum, then to line coalescence with broad, unstructured features and finally to the re-emergence of a quadrupole doublet having a reduced effective splitting and a decreasing line width (motional narrowing). This reduced splitting is smaller for 60° as compared with 30° and 90°: for fast rotation, the average EFG is effectively reduced to $V_{zz}(1 - 3\cos^2\vartheta)$, i.e. it passes through zero at the "magic angle" known from solid-state NMR ($\vartheta = 54.7356°$). Only numerical calculations are possible for the Blume jump models in the general case so that no least-squares fitting of experimental data is possible.

Recently, a model for completely random angular jumps of the azimuthal angle φ [8] was developed within a modified Blume-type formalism [11], yielding a closed analytical expression. We call this model the random jump cone (RJC) model. Fits of the resonant cross-section

of the Blume jump models by means of the RJC model produced a perfect matching of the spectral shape, plus average cone opening angles equal to the ones of the Blume models, with the exception of small relaxation rates for models D and F. In these two cases, also the ratio $\lambda/3W$ – where λ is the RJC jump rate and W is the jump rate that appears in the Blume jump matrix – deviates from the value $\lambda/3W = 1$ as given in [10] for the isotropic random jump model, oscillating for slow relaxation but approaching a constant value for fast relaxation. Obviously, both the 3-jump models and the RJC model imply that each EFG orientation can be reached from each other one with equal probability, which is not the case for the out-of-plane 6-jump models.

Finally, the RJC model contains an ambiguity for Mössbauer or NFS spectra, as the fit parameter $\alpha = \frac{1}{2}(3\cos^2\vartheta - 1)$ enters the resonant amplitude as α^2 for the range $0 \leq \alpha \leq 0.5$ (the valid range of α is $-0.5 \leq \alpha \leq 1$). This ambiguity can be removed using complementary SRPAC data, see the next Sections.

The dependence of dynamics on SRPAC time spectra has been developed in [3]. For the strong-collision model, slow rotation entails a damping of the QB and an increased slope of the QB envelope. For fast rotation, a separate determination of quadrupole splitting and rotation time is no longer possible. The RJC model gives analytical solutions in the slow and fast relaxation limit [8]. In contrast to MS or NFS, there is no ambiguity concerning the sign of α.

3. Experiments

SSZ-24, prepared according to [12], was loaded by the same procedure as used for $AlPO_4$-5 [4]. Samples with a natural isotope distribution and samples enriched in ^{57}Fe were prepared simultaneously under precisely identical conditions. The enriched samples were used for the MS and NRS experiments and characterized *a posteriori*. The non-enriched samples were characterized in their freshly prepared state for comparison, see [6]. The MS and NRS measurements were done on fresh samples. The bulbs with the sealed samples were opened directly before the NRS experiments. For the sake of comparison, also MS measurements on the samples previously investigated at the synchrotron were carried out.

The Mössbauer measurements were performed in a He bath cryostat with source and absorber in liquid He. Measurements for rising temperatures were done during a slow two-step warm-up process of the cryostat, where source and absorber were kept at the same temperature within the range of 30–290 K. The source was a standard 50 mCi ^{57}Co/Rh source as delivered by Ritverc (Russia).

NFS and SRPAC can be conveniently carried out simultaneously using the standard experimental setup for NRS experiments. Those were done at the beamline ID18 of the ESRF [13]. The primary beam ($\Delta E = 3.5$ meV) was provided by a nested four-bounce high-resolution monochromator [14, 15]. The samples were mounted into a copper holder sealed with kapton windows, within a closed-cycle cryostat having a temperature stability of ± 1°C, for the low-temperature measurements, and into a small high-temperature oven for measurements above room temperature. In order to protect ferrocene from oxidation at elevated temperatures but also to prevent its sublimation into the isolation vacuum, the oven was slowly flushed with a N_2 gas stream throughout the experiment.

Time spectra were taken mostly in four-bunch mode in a time window of 704.14 ns. The temperature was varied from 50 K to 505 K. Note that the bulk melting temperature for ferrocene is reported as 446 K. For the $AlPO_4$-5 system, owing to lower loading and hence low count rates, no SRPAC data above room temperature were recorded.

4. Results and discussion

Mössbauer spectra of ferrocene in SSZ-24 at three different temperatures are shown in Fig. 3. The fit to all MS data was done using the transmission integral [16]. In addition to the quadrupole

doublet observed at low temperatures, a second doublet having reduced splitting emerges with rising temperature and finally dominates the spectrum. We suggest that the four-line spectra can be ascribed to an equilibrium between mobile and immobile species. For temperatures below 100 K, almost all ferrocene molecules are stationary. With rising temperature, the intensity of the inner doublet increases, i.e. an increasing percentage of molecules become unlocked and starts to rotate.

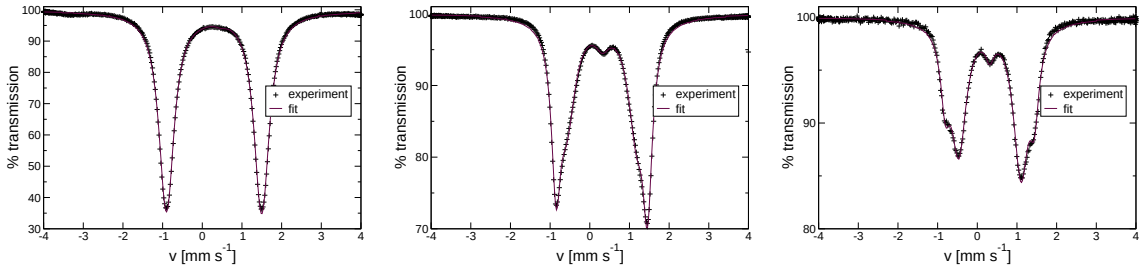

Figure 3. Mössbauer spectra of ferrocene in SSZ-24 at 4 K (left), 173 K (centre) and 225 K (right), assuming a line width of the source of 0.15 mm s^{-1}.

Examples of NFS and SRPAC time spectra of ferrocene in SSZ-24 are shown in Fig. 4. In NFS, the emerging "inner" doublet modulates coherently the quantum beat of the "outer" doublet with increasing temperature. For the SRPAC spectra, first an apparent disappearance of the QB of the "outer" doublet and then an apparent emergence of the QB of the "inner" doublet having a reduced frequency are observed. The frequency of this QB amounts to about 25 % of the original one, as the beats from both species sum incoherently. Because of the "fast" QB decay of the inner doublet, the QB structure at low temperatures is entirely dominated by the "outer" doublet. This effect diminishes as the relative intensity of the "outer" doublet decreases at higher temperature.

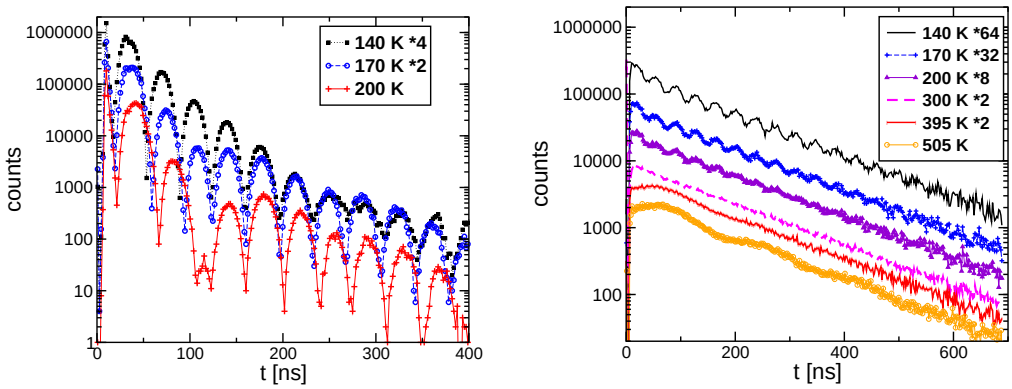

Figure 4. NFS (left) and SRPAC (right) time spectra of ferrocene in SSZ-24 at different temperatures. For the ease of comparison, spectra at low temperatures have been offset/multiplied as indicated in the legends.

We associate the relative integrated intensities of "outer" and "inner" doublet with the quantity of stationary (n_1) and mobile (n_2) species and set up a van't Hoff plot of the equilibrium constant $K = n_2/n_1$ versus $1/T$, see Fig. 5. The fairly linear behaviour supports our assumption of an equilibrium between stationary and mobile species. The fit yields $\Delta H = (8.17 \pm 0.07)\,\mathrm{kJ\,mol^{-1}}$ and $\Delta S = (47.0 \pm 0.4)\,\mathrm{J\,mol^{-1}\,K^{-1}}$.

Owing to the f_{LM}^2 decay of the NFS intensity with temperature, the statistics of high-temperature NFS data of dynamical systems is often limited. Moreover, the complicated analytical form of the RJC model makes it impossible to treat multiple scattering properly by fitting (for a discussion of the treatment of co-existing multiple scattering and dynamics in a somewhat simpler case cf. [17]). However, it is possible to carry out a consistency check as follows. Among other features, dynamics always leads to an enhanced signal decay in the time domain $\mathrm{e}^{-t/\tau}$, which can be converted into a line broadening $\Delta\omega$ in the energy domain by $\Delta\omega = \hbar/\tau$. A comparison of MS and NFS line broadenings thus obtained is shown in Table 1. The kinematical fit was done using the RJC model neglecting multiple scattering; the dynamical fit was done using the Motif software [18], which treats multiple scattering correctly, but only includes dynamics as a simple exponential decay. The absolute values as obtained by the different methods agree with each other within experimental accuracy, indicating that the MS and NFS data are indeed mutually consistent.

A fit using the four-jump in-plane Blume-type model [5] does not yield a satisfactory agreement between theory and experiment for MS or NFS spectra. Always the width of the inner doublet is overestimated (which was also discussed but not resolved in [5]). We fitted all experimental data using the RJC model (including an asymmetry factor for the quadrupole doublets) and obtained a good description of the Mössbauer line shape.

A comprehensive Arrhenius plot for MS and SRPAC data on the ferrocene/SSZ-24 system is shown in Fig. 6. The plot includes MS measurements of both the sample studied at the synchrotron (sample 1) and another sample prepared separately (sample 2), so as to obtain an indication for the size of the true experimental error, compared to the fit errors which, sometimes depending on software, tend to be smaller than the true experimental error.

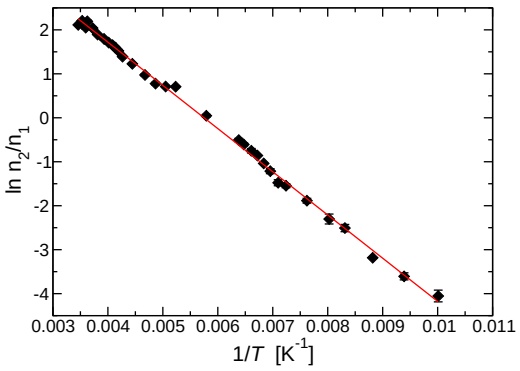

Figure 5. Van't Hoff plot of ferrocene in SSZ-24.

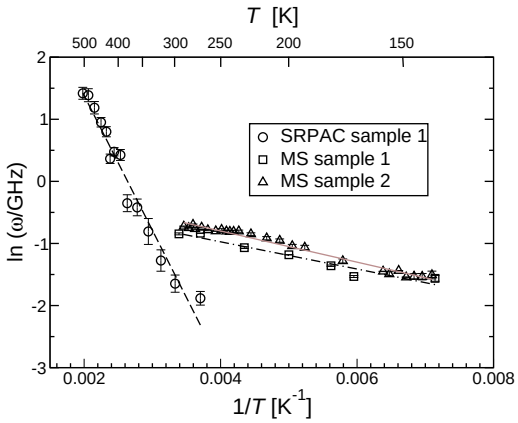

Figure 6. Arrhenius plot, including fitting, of the relaxation rates for ferrocene in SSZ-24 for MS and SRPAC. Fit errors are in the range of size of the symbols.

In the temperature range from 140 K to 290 K, we obtained an activation energy of $E_a = (1.8\pm0.2)\,\mathrm{kJ\,mol^{-1}}$. Low activation energies have been observed using solid state NMR for reorientational motion in inclusion compounds containing aromatic species [19]. The very low frequency factor – $A = (9.1\pm0.1)\cdot10^8\,\mathrm{s^{-1}}$ – suggests that the dynamics can probably not be described by a single activated jump in this temperature regime, but that an additional process mimicks apparent Arrhenius parameters [20].

The SRPAC data were fitted using the high-temperature approximation of the RJC model. The Arrhenius parameters for the two methods and temperature regimes differ strongly. For the SRPAC data they are $E_a = (20.1\pm0.8)\,\mathrm{kJ\,mol^{-1}}$ and $A = (5.5\pm1.6\cdot10^{11})\,\mathrm{s^{-1}}$. In particular, the

activation energy exceeds the one obtained from the MS data by more than a factor of six, and the large frequency factor, which is consistent with an entire-molecule rotation, indicates the presence of a single activated process. As ϑ increases strongly with temperature, cf. Fig. 7, it appears plausible that this increase will also enhance the activation energy of the corresponding jump rotation. The ϑ values as obtained from both MS and SRPAC fit together in the overlap region, indicating the consistency of these two methods as well.

Table 1. Line broadening of the inner doublet (in units of Γ) for NFS and MS data on ferrocene in SSZ-24, for details see text.

T [K]	NFS kinematical	NFS dynamical	MS
170	3.16 ± 1.04	3.46	3.84 ± 0.08
200	3.71 ± 1.01	3.32	3.32 ± 0.06
230	3.52 ± 1.11	2.96	3.29 ± 0.01
270	3.66 ± 0.54	2.90	3.97 ± 0.05
300	4.59 ± 0.99	4.25	4.08 ± 0.04

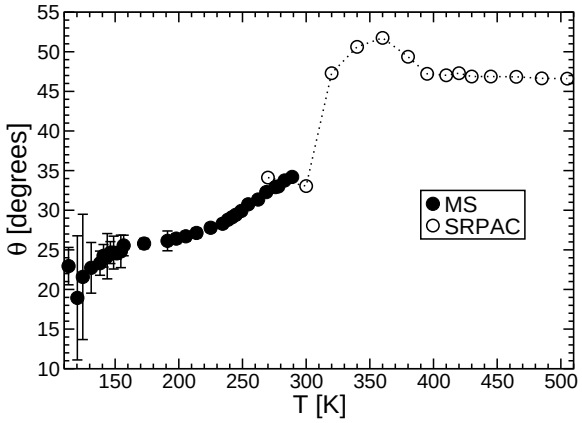

Figure 7. Average cone opening angle ϑ using the RJC model for ferrocene in SSZ-24.

Before deciding in favour of a particular jump model, one has to take into account that MS "sees" all types of motion, whereas SRPAC is exclusively selective to the rotational part, which may in part explain the somewhat different relaxation rates around 300 K as observed by MS/NFS and SRPAC. Moreover, different rotational jump models – as discussed above – may yield very similar activation energies but influence the absolute scaling of relaxation rates and thus also the gap in relaxation rates as seen by different methods.

5. Conclusions and outlook

A combination of classical Mössbauer spectroscopy and nuclear resonant scattering provides comprehensive information about anisotropic molecular rotation in a wide dynamic range. We observe anisotropic jump rotation with rising temperature in both systems $AlPO_4$-5 and SSZ-24, where the molecular axis of included ferrocene preferentially appears to reorient on a cone.

Although the RJC model gives a good overall description of the experimental data, a detailed inspection gives hints that the true jump mechanism may be more complex. We speculate that the jump rotation may weakly couple to small translational jumps of the ferrocene molecules within the host cages.

For $AlPO_4$-5, the MS data show a similar picture as for SSZ-24 in the low-temperature range, with altogether slower dynamics. An additional study of the system ferrocene/oriented $AlPO_4$-5 single crystals has been carried out [6] using SYNFOS [21], supporting the suggestion that translation-rotation coupling may have to be treated by more sophisticated theoretical models still to come.

In contrast to methods that are selective to the movements of e.g. the hydrogen nuclei, including complicated motions of mobile groups such as methyl rotations, SRPAC yields exclusively the rotation of the electric field gradient, which is usually associated with the motion of the *entire* molecule. This technique is thus complementary to NMR or neutron scattering.

References

[1] J Kärger, and D M Ruthven 1992 *Diffusion in Zeolites and Other Microporous Solids* (New York: Wiley)
[2] NY Chen, TF Degnan, Jr., and CM Smith 1994 *Molecular Transport and reaction in zeolites* (Weinheim: VCH)
[3] I Sergueev, U van Bürck, A. I Chumakov, T Asthalter, G. V Smirnov, H Franz, R Rüffer, and W Petry 2006 *Phys. Rev. B* **73** 024203
[4] T Asthalter, J Villanueva Garibay, V Olszowka and J Kornatowski 2005 *J. Chem. Phys.* **122** 014508
[5] T. C Gibb 1976 *J. Phys. C: Solid State Phys.* **9** 2627
[6] T Asthalter 2007 *Habilitationsschrift* (Stuttgart)
[7] M Blume 1968 *Phys. Rev.* **174** 351
[8] I Sergueev, T Asthalter, and U van Bürck, unpublished
[9] J,A Tjon, and M Blume 1968 *Phys. Rev.* **165** 456
[10] S Dattagupta, and M Blume 1974 *Phys. Rev. B* **10** 4540
[11] S Dattagupta, and K Schroeder 1987 *Phys. Rev. B* **35** 1527
[12] R Bialek, W. M Meier, M Davis, and M. J Annen 1991 *Zeolites* **11** 438
[13] R Rüffer, and A. I Chumakov 1996 *Hyperfine Int.* **97/98** 589
[14] T Toellner 2000 *Hyperfine Int.* **125** 3
[15] T Ishikawa, Y Yoda, K Izumi, C K Suzuki, X,W Zhang, M Ando, and S Kikuta 1992 *Rev. Sci. Instrum.* **63** 1015
[16] I Sergueev, personal communication.
[17] I Sergueev, H Franz, T Asthalter, W Petry, U van Bürck, and G. V Smirnov 2002 *Phys. Rev. B* **66** 184210
[18] Y V Shvydko 2000 *Hyperfine Int.* **125** 173
[19] JA Villanueva-Garibay, and K Müller 2006 *Phys. Chem. Chem. Phys.* **8** 1394
[20] DVujosevic, KMüller, and E Roduner 2006 *J. Phys. Chem. B* **110** 8598
[21] M Haas, E Realo, H Winkler, W Meyer-Klaucke and AX Trautwein 2000 *Hyperfine Int.* **125** 189